OXIDATIVE STABILITY OF BIODIESEL BY DYNAMIC MODE PRESSURIZED-DIFFERENTIAL SCANNING CALORIMETRY (P-DSC)

R. O. Dunn

ABSTRACT. *Biodiesel, an alternative diesel fuel made from transesterification of vegetable oils or animal fats, is composed of saturated and unsaturated long−chain fatty acid alkyl esters. During long−term storage, oxidation caused by contact with ambient air presents legitimate concerns for monitoring fuel quality. Extended oxidative degradation can affect kinematic viscosity, cetane number, and acid value of the fuel. This work investigates the suitability of dynamic mode (positive air purge) pressurized−differential scanning calorimetry (P−DSC) as a means for evaluating the oxidation reaction during non−isothermal heating scans. Methyl oleate, methyl linoleate, and soybean oil fatty acid methyl esters (FAME) were analyzed by P−DSC and the results compared with those from thermogravimetric analyses (TGA), conventional DSC, and static mode (zero purge gas flow) P−DSC scans. Results from TGA showed that ambient air pressure was too low to allow measurable oxidation during analyses. Although some degree of oxidation was detected for DSC and static mode P−DSC heating scans, results demonstrated that the highest degree of oxidation occurred during dynamic mode P−DSC scans. For DSC and P−DSC analyses, oxidation onset temperature (OT) increased with relative oxidative stability, with the highest values being observed for methyl oleate. Treating soybean oil FAME with antioxidants increased their relative oxidative stability, resulting in an increase in OT. Statistical comparison of response factors (R_F) relative to methyl oleate obtained from non−isothermal heating scans with those obtained from OSI analyses showed the highest degree of correlation (P = 0.79) with respect to dynamic mode P−DSC.*

Keywords. *Antioxidant, Diesel fuel, Differential scanning calorimetry, Fatty acid methyl esters, Oil stability index, Onset temperature, Soybean oil, Thermogravimetric analysis.*

Biodiesel (fatty acids alkyl esters derived from agricultural lipids) is an alternative fuel or extender for combustion in compression−ignition engines. Many applications such as trucks and automobiles, farm vehicles and tractors, locomotives, aircraft, stationary power, and heat generation have been proposed. Biodiesel has the following favorable characteristics: (1) it is made from renewable domestic feedstocks; (2) it is environmentally innocuous and relatively biodegradable; (3) it is non−flammable (relatively high flash point) and safe to handle; (4) it has energy content, specific gravity, kinematic viscosity, and cetane number comparable to petroleum middle distillate fuels (petro−diesel); (5) it enhances lubricity and improves antiwear properties in blends with petro−diesel; and (6) it yields in excess of three times the energy required to produce it and has a net−negative carbon dioxide balance (Knothe and Dunn, 2001; Graboski and McCormick, 1998; Sheehan et al., 1998; Krahl et al., 1996a; Krahl et al., 1996b; Van Gerpen et al., 1996). A recent comprehensive analysis conducted by the U. S. Environmental Protection Agency (U.S. EPA, 2002) concluded that biodiesel significantly reduces regulated exhaust emissions of unburned hydrocarbons, carbon monoxide, and particulate matter at all blend levels with petro−diesel. Biodiesel also decreases emissions of smoke opacity, sulfur dioxide, aldehydes, ketones, and polycyclic aromatic hydrocarbons (Knothe and Dunn, 2001; Graboski and McCormick, 1998; Krahl et al., 1996a; Krahl et al., 1996b). Its main disadvantages are relatively poor cold flow properties, degradation of fuel quality during long−term storage, and its combustion slightly increases nitrogen oxides emissions.

Storage stability is generally defined as the relative resistance of a liquid fuel to physical and chemical changes brought about by interaction with its environment (Westbrook, 2003). Stability takes into account interactions that lead to sediment formation and changes in color depending on the type and quantity of unstable materials present. Cleanliness relative to presence of water, particulate solids, degradation products, and microbial slimes can also influence stability (Giles, 2003). Fuel properties degrade during storage due to effects of oxidation (autoxidation) from contact with ambient air, thermal or thermal−oxidative decomposition from excess heat, hydrolysis from contact with moisture in tanks and fuel lines, or microbial contamination from migration of dust particles or water droplets containing bacteria or fungi (Giles, 2003; Westbrook, 2003). This work examines effects of oxidation on biodiesel storage stability.

Submitted for review in November 2005 as manuscript number BE 6215; approved for publication by the Biological Engineering Division of ASABE in August 2006.

Mention of brand or firm name does not constitute an endorsement by USDA over others of a similar nature not mentioned.

The author is **Robert O. Dunn,** Chemical Engineer, Food and Industrial Oils Research, USDA−ARS National Center for Agricultural Utilization Research, Peoria, Illinois; phone: 309−681−6101; fax: 309−681−6340; e−mail: dunnro@ncaur.usda.gov.

Most common lipid feedstocks consist of triacylglycerols with long−chain fatty acid groups. Biodiesel made from feedstocks with very high concentrations of C_{14+} fatty acid groups should have no less than 80 to 90 wt% unsaturated (low melting point) fatty acid alkyl esters because small quantities of saturated (high melting point) fatty acid alkyl esters can significantly influence cold flow properties (Dunn, 2005a; Dunn and Bagby, 1995). On the other hand, unsaturated organic compounds are substantially more reactive to oxidation than saturated compounds with the same hydrocarbon chain length. Furthermore, polyunsaturated compounds are more reactive than monounsaturated compounds (Gunstone, 1967).

Monitoring effects of oxidative degradation on fuel quality during long−term storage presents a legitimate concern for biodiesel producers, suppliers, and consumers (Stavinoha and Howell, 1999). Assessing quality in accordance with fuel standards, such as ASTM Specification D 6751 (ASTM, 2003), for biodiesel is rigorous and time consuming. Oxidation of biodiesel under accelerated conditions such as elevated temperature and purging with dry air or oxygen increases viscosity, acid value, and peroxide value (Dunn, 2002; Monyem et al., 2000; Thompson et al., 1998; Bondioli et al., 1995; Du Plessis et al., 1985). Both viscosity and acid value have maximum limits specified in D 6751. Although peroxide value is not listed, increasing the concentration of hydroperoxides actually increases cetane number, a parameter that is listed in ASTM Specification D 6751. Increasing peroxide value may reduce ignition delay time of the fuel (Van Gerpen, 1996; Clothier et al., 1993). However, extensive oxidative degradation causing decomposition of hydroperoxides eventually decreases peroxide value and cetane number, leading to an increase in ignition delay time (Dunn, 2002; Monyem et al., 2000; Gan et al., 1995; Miyashita and Takagi, 1988).

There exists a need to develop analytical methods for rapid and accurate monitoring of biodiesel fuel quality with respect to effects of oxidation degradation during storage. The recently completed BIOSTAB project in Europe was undertaken to establish criteria and analytical methods for measuring biodiesel fuel stability (Bondioli et al., 2002; Mittelbach and Schober, 2003; Prankl, 2002; Lacoste and Lagardere, 2003). The resulting unified standard method drafted for adoption in the European Union states is based on the analysis of oxidation induction period at 110°C by Rancimat method. However, the BIOSTAB studies were largely conducted on biodiesel whose feedstock oil had relatively low polyunsaturated fatty acid methyl esters (FAME) content (rapeseed oil, used cooking oils, etc.). Earlier work (Dunn and Knothe, 2003) and Canakci et al. (1999) recommended a block temperature no greater than 60°C for measurement of induction period by oil stability index (*OSI*) analyses of soybean oil FAME (SME) to avoid rapid degradation at higher temperatures.

Thermal analytical methods such as thermogravimetric analysis (TGA), conventional differential scanning calorimetry (DSC), and pressurized−differential scanning calorimetry (P−DSC) have been applied in analyzing oxidation of petroleum−based and synthetic lubricants, biodegradable lubricants, aviation turbine oils, and polymers (Sharma and Stipanovic, 2003; Gamelin et al., 2002; Riga et al., 1998; Yao, 1997; Zeman et al., 1995; Zeman et al., 1993). These studies showed that P−DSC has the advantage of increased number of moles of oxygen available for reaction, allowing acceleration of the reaction at lower temperatures. Stavinoha and Kline (2001) applied ASTM Method D 6186 (Oxidation induction time of lubricating oils by pressure differential scanning calorimetry) and reported that this method was suitable for monitoring and spot−checking oxidative stability of antioxidant−treated biodiesel. An earlier study (Dunn, 2005b) demonstrated suitability of non−isothermal (temperature ramping) P−DSC analyses for determining effects of antioxidant type and concentration (loading) on oxidative stability of biodiesel. Finally, Litwinienko and Kasprzyska−Guttman (2000) and Litwinienko et al. (1999, 2000) applied non−isothermal DSC and P−DSC analysis to study the kinetics of oxidation of long−chain (C_{18}) unsaturated FAME and fatty acid ethyl esters.

The present work investigates the suitability of thermal analysis by non−isothermal TGA, conventional DSC, and P−DSC analyses on oxidation of SME. Results from thermal−oxidative methods are compared with each other, including comparison of P−DSC analyses in static (zero purge gas flow) and dynamic (positive air flow) modes. Results were also compared with those from isothermal analysis of *OSI*. Effects of treating SME with added antioxidant are examined.

Materials and Methods

Methyl esters of soybean oil fatty acids (SME) were acquired from the following two sources: (1) "SME−1," originally manufactured by Interchem (Overland Park, Kansas) and supplied by the National Biodiesel Board (NBB, Jefferson City, Mo.); and (2) "SME−2," directly acquired from Ag Environmental Products (Lenexa, Kansas). Gas chromatographic (GC) analyses indicated a fatty acid profile of 10.7 wt% palmitate, 3.6% stearate, 22.8% oleate, 55.4% linoleate, and 7.5% linolenate for SME−1. Analysis of the fuel properties of SME−1 yielded kinematic viscosity = 4.1 mm^2/s at 40°C, acid value = 0.16 mg KOH/g, specific gravity = 0.8813 at 15.6°C, and cloud point = 0°C. GC analyses of SME−2 showed a fatty acid profile of 11.2% palmitate, 4.1% stearate, 25.0% oleate, 52.6% linoleate, and 7.0% linolenate, plus a trace concentration (<0.1%) of methyl arachidate. Fuel properties of SME−2 were kinematic viscosity = 4.2 mm^2/s at 40°C, acid value = 0.22 mg KOH/g, specific gravity = 0.8863 at 15.6°C, and cloud point = 1.5°C. According to the fuel manufacturers, neither SME−1 nor SME−2 contained added oxidation inhibitors (antioxidants). Methyl oleate (+99% 9(Z)−octadecenoic acid methyl ester) and linoleate (+99% 9(Z),12(Z)−octadecadienoic acid methyl ester) were from Nu Chek Prep (Elysian, Minn.). Purity of both compounds was verified by GC. Antioxidants ±α−tocopherol (95%) and propyl gallate (97% 3,4,5−trihydroxybenzoic acid propyl ester) were from Aldrich (Milwaukee, Wisc.); *tert*−butylhydroquinone (TBHQ; 97%), BHA (9% 2−*tert*−butyl−4−hydroxyanisole, 90% 3−*tert*−butyl−4−hydroxyanisole), and BHT (99% 2,6−di−*tert*−butyl−4−methylphenol) were from Sigma (St. Louis, Mo.).

TGA Analyses

Non−isothermal TGA was employed to measure the effects of constant temperature increase (heat ramping) on the mass of the sample while it is being purged with air at

ambient pressure. These analyses were conducted with a TA Instruments (New Castle, Del.) model Q500 TGA equipped with automated gas switching and mass flowmeter. Experimental control, data acquisition, and analyses of results were conducted with a model 5000 personal computer–based controller. Samples were placed in an open aluminum pan equipped with a wire handle and hooked into place in the opened TGA assembly. Once placed on the hook, the TGA oven was raised to envelop the pan, and the sample equilibrated under low–pressure nitrogen purge at 25˚C. Purge gas flowrate was 60 mL/min, as set according to manufacturer's recommendation and monitored automatically by the Q500 TGA during each scan. After equilibrating at 25˚C, the sample was heated at 5˚/min to 300˚C to ensure mass loss in the range 85% to 90%. During some scans, purge gas was switched automatically from nitrogen to air before initiating the heat ramp. Sample mass for TGA scans was 15 ±2.2 mg.

Conventional DSC and P-DSC Analyses

Conventional DSC was employed in the current study to analyze effects of thermal–oxidation induced by rapidly increasing temperature (heat ramping) on heat flow through a sample exposed to an air atmosphere at ambient pressure. Analogously, static and dynamic mode P–DSC were used to analyze effects of heat ramping when the sample is exposed to an air atmosphere under 2000 ±50 kPa (290 ±7 psig) pressure. Heating scans were conducted using two hermetically sealed aluminum pans with a 0.5 mm diameter pinhole punched in the top cover, allowing direct contact with the air inside the measurement cell. One empty pan served as the reference pan, while the sample to be analyzed was placed in the second pan. Heat flow through the sample was then determined by subtracting heat flow through the reference pan from that through the sample pan. The hermetic pans with pre–punched holes in their lids were used for two reasons: (1) tests with open solid fat index (SFI) type pans caused a build–up of varnish deposits inside the cell (Dunn, 2000), and (2) closed type pans have been shown to minimize diffusion effects that can interfere with analyses (Keller and Saba, 1998).

All DSC and P–DSC analyses were conducted with a TA Instruments model 2910 DSC analytical module and the same model 5000 multi–tasking controller used for TGA analyses. (The model 5000 controller was actually capable of performing control, acquisition, and data analysis simultaneously for up to eight compatible analytical modules.)

DSC analyses at ambient pressure were conducted with the "conventional" DSC cell installed on the analytical module. Gas flowrate through the cell was 75 mL/min, as recommended by the manufacturer and monitored by calibrated flowmeter. After loading the DSC cell with both reference and sample pans, the cell was closed and equilibrated at 25˚C under nitrogen gas purge. Once the cell and its contents were equilibrated, purge gas was automatically switched to air and the cell heated at 5˚/min to 195˚C to ensure acquisition of an oxidation peak maximum. Sample mass for these scans was 2.1 ±0.80 mg.

Both static and dynamic mode P–DSC analyses under 2000 kPa pressure were conducted with a TA Instruments model 2910 HP–DSC cell (7 MPa maximum pressure) installed on the analytical module. A spring–action purge valve was fitted to the exhaust line to keep the cell at constant pressure during analysis. For static mode scans, after loading the sample and reference pans and clamping the corresponding cell lid into place, the cell was pressurized with dry air and sealed off. Once the pressurized cell and its contents were equilibrated at 25˚C, the sample was heated at 5˚/min to 175˚C to ensure acquisition of an oxidation peak maximum. Sample mass for static mode scans was 2.8 ±0.49 mg.

For dynamic mode P–DSC scans, pans were loaded and the cell pressurized and sealed similar to operating in static mode. Once cell pressure equilibrated, the inlet valve was opened wide and the outlet valve was cracked slightly open to allow steady flow of air through the cell. Air flowrate was set manually to 35 ±3 mL/min and monitored by a calibrated gas flowmeter connected downstream from the cell outlet valve. Once air flow was established and pressure re–stabilized, the cell and its contents were equilibrated at 25˚C and the sample heated at ramp rate = 5˚/min to 195˚C to ensure acquisition of an oxidation peak maximum. Sample mass for dynamic mode scans was 1.5 ±0.36 mg.

DSC and P–DSC scans produced curves such as those shown for analysis of SME–1 in figure 1. Curves were analyzed by the model 5000 controller to determine *OT* from the intersection of lines drawn tangent to the initial baseline and the point of maximum increase (that is, the point of inflection) in the oxidation peak. *OT* results reported in this work are means calculated from scans performed on three replicate samples.

OSI Analyses

OSI data were measured isothermally in an oxidative stability instrument from Omnion, Inc. (Rockland, Mass.) under license from Archer Daniels Midland (Decatur, Ill.). This instrument was employed to measure oxidation induction period at constant temperature. Induction period, defined as being equivalent to *OSI*, is the time period necessary for oxidative degradation to advance from forma–

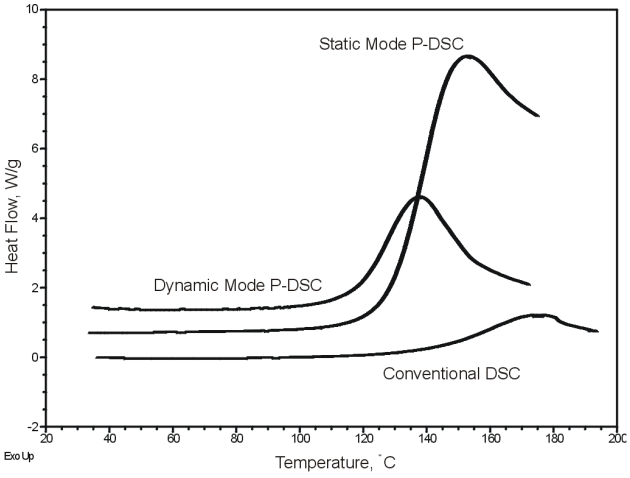

Figure 1. Heating scans from conventional differential scanning calorimetry (DSC) and static and dynamic mode pressurized (P)–DSC analyses of SME–1 (soybean oil fatty acid methyl esters [FAME] from Interchem). For P–DSC: air flowrate = 35 mL/min in dynamic mode (only); pressure = 2000 kPa; ramp rate = 5˚C/min. For DSC: air flowrate = 75 mL/min; pressure = ambient; ramp rate = 5˚C/min. Analysis of curves yielded oxidation: (1) onset temperature (*OT*) = 136.60˚C for DSC, 124.78˚C for static mode P–DSC, and 115.94˚C for dynamic mode P–DSC; and (2) peak maximum temperature = 174.66˚C for DSC, 153.34˚C for static mode P–DSC, and 137.66˚C for dynamic mode P–DSC.

tion of primary products (hydroperoxides) to secondary products such as aldehydes, ketones, small–chain length hydrocarbons, polymers, and volatile organic acids. The analytical method employed in the current study was reported in an earlier work (Dunn, 2005c). Prior to analysis, samples were vacuum distilled at 60˚C and 0.05 to 0.10 mm Hg absolute pressure for 3 h in a Kugelrohr apparatus (Aldrich) to remove volatile contaminants that may interfere with analysis. In the present work, all samples were analyzed at block temperature = 60 ±0.2˚C. Sample mass for *OSI* measurement was 5 g.

Gas Chromatography Analyses

Fatty acid compositions of SME–1 and SME–2 were performed on a Perkin Elmer (Norwalk, Conn.) Autosystem GC with a 25 m × 0.32 mm ID BPX70 column from SGE (Austin, Texas). The temperature program was: (1) hold 5 min at 50˚C, (2) ramp at 10˚/min to 250˚C, and (3) hold 10 min at 250˚C. Follow–up analyses of SME–2 were performed on an Agilent Technologies (Palo Alto, Cal.) model 6890N GC equipped with an HP–5MS capillary column (30 m × 0.25 mm ID; 0.5 μm film) and coupled with a model 5973N mass selective detector operating in electron ionization mode at 70 eV. Library searches to aid in identifying components of biodiesel were performed using the Wiley Library provided by Agilent Technologies.

Regression and Statistical Analysis of Results

Least–squares linear regression analyses including analysis of variance (ANOVA) and comparison of mean values by Student's t–value methods were conducted using a standard personal desktop computer–based spreadsheet application.

Results and Discussion

TGA

Results from non–isothermal TGA analyses of methyl oleate, SME–1, and SME–2 are summarized in table 1. Onset temperatures (*OT*) for SME–1 under air and nitrogen atmospheres exhibited very high probability (P = 0.886) of being equivalent to each other. Similar conclusions were drawn from comparison of temperature at maximum in the first derivative of the mass–temperature curves and total mass lost data for SME–1 and for *OT*, first derivative, and total mass lost data for methyl oleate. Ramping under nitrogen purge gas causes thermal degradation to dominate mechanisms associated with decomposition and loss of mass during analysis. The near equivalence between results under nitrogen and air purge gases suggests that little oxygen was consumed during analyses under the air purge. Therefore, an air atmosphere at ambient pressure and purge rate of 60 mL/min did not provide a sufficient quantity of oxygen to promote measurable oxidative degradation during analysis. It is apparent that non–isothermal TGA will be more suitable for analyzing thermal stability characteristics of biodiesel rather than its relative oxidative stability.

Table 1. Results from non–isothermal thermogravimetric analysis (TGA) of fatty acid methyl esters (FAME) under air and nitrogen purge gas (air flowrate = 60 mL/min; ramp rate = 5˚C/min).[a]

FAME	Purge Gas	*OT* (°C)	T_{MFD} (°C)	*M* (%)
Methyl oleate	Nitrogen	194 ±2.3	232 ±3.7	91 ±2.5
Methyl oleate	Air	192 ±2.1	230 ±2.6	90 ±1.7
SME–1	Nitrogen	189 ±3.6	225 ±5.0	90 ±5.1
SME–1	Air	189 ±2.8	222 ±3.1	87 ±1.0
SME–2	Nitrogen	194 ±3.1	229 ±3.0	92 ±1.9

[a] SME–1 = soybean oil FAME from Interchem, SME–2 = soybean oil FAME from Ag Environmental Products. *OT* = onset temperature, T_{MFD} = temperature at maximum in the first derivative of the mass loss–temperature curve, and *M* = total mass lost during the reaction.

Dynamic Mode P–DSC

Figure 2 is a graph of dynamic mode P–DSC heating curves for SME–1, SME–2, and methyl oleate. Each of these curves exhibit onset (*OT*) and peak maximum temperatures detected at heating scan rate of 5˚C/min. Methyl oleate yielded *OT* and peak temperature at higher values than those for either SME–1 or SME–2, indicating that this FAME was more stable during non–isothermal P–DSC heating curve analysis. This aligns well with methyl oleate having a higher oxidative stability relative to FAME composed of high concentrations of polyunsaturated hydrocarbons.

Comparing results for the SMEs in figure 2, *OT* occurs at a significantly higher temperature for SME–2 (130.94˚C) than for SME–1 (115.94˚C). Given the similar fatty acid compositions for these two SME (see above), this suggested that either SME–1 was more harshly handled during the time prior to its selection for the current study or SME–2 contained a small concentration of antioxidants. GC–MS analysis of SME–2 against a series of antioxidant reference samples failed to detect the presence of antioxidants including ascorbic acid, BHA, BHT, citric acid, ethoxyquin, propyl gallate, TBHQ, 3,3–thiopropionic acid, α–tocopherol, δ–tocopherol, or trihydroxybutyrophenone. Thus, it appears likely that SME–1 was more harshly treated prior to its selection for the current work.

Dynamic Mode P–DSC Versus Conventional DSC

Results from conventional DSC and dynamic mode P–DSC analyses of methyl oleate, methyl linoleate, SME–1, SME–2, and SME–1 treated with 2000 ppm each of antioxidants α–tocopherol and TBHQ are summarized in table 2. Response factors (R_F) defined by the following ratio are also summarized:

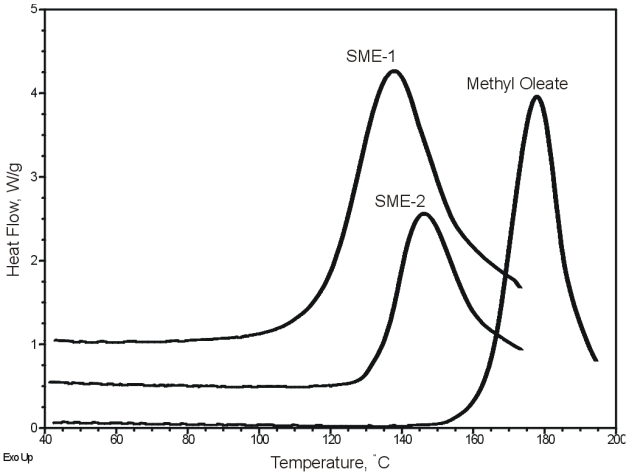

Figure 2. Heating scans from dynamic mode P–DSC analyses of FAME (air flowrate = 35 mL/min; pressure = 2000 kPa; ramp rate = 5˚C/min). SME–2 = soybean oil FAME from Ag Environmental Products. Analysis of curves yielded: (1) *OT* = 115.94˚C for SME–1, 130.94˚C for SME–2, and 162.70˚C for methyl oleate; and (2) peak maximum temperature = 137.66˚C for SME–1, 145.97˚C for SME–2, and 177.90˚C for methyl oleate. See figure 1 for abbreviations.

$$R_F = [OT \text{ of sample}]/[OT \text{ of methyl oleate}] \quad (1)$$

where *OT* of sample and methyl oleate are measured by corresponding analytical techniques. For FAME not treated by added antioxidants, the results in table 2 consistently show that increasing the degree of unsaturation decreases *OT* from non−isothermal thermal analysis by DSC or P−DSC, which is in agreement with the notion that *OT* increases with increasing FAME oxidative stability. Only SME−1 was treated with added antioxidants in the present work. Increasing the oxidative stability of SME−1 by adding 2000 ppm antioxidant also resulted in a significant increase in *OT*. Comparing the antioxidants, TBHQ was more effective than α−tocopherol with respect to increasing *OT*, a result that generally agreed with those reported in an earlier antioxidant screening study (Dunn, 2005b).

Although results for methyl oleate show ~4°C deviation between *OT* values from DSC and dynamic mode P−DSC, statistical comparison of the values in table 2 did not indicate significant deviation between these values ($P = 0.23$). However, similar comparisons for methyl linoleate, SME−1 with and without added antioxidant, and SME−2 revealed deviations that were significant ($P < 0.05$). The dynamic mode P−DSC analyses were conducted at higher pressure (2000 kPa vs. ambient for DSC) and lower air purge rate (35 vs. 75 mL/min). The increase in pressure increased the total oxygen mass available for reaction by a factor of 19.7, a condition that accelerates the oxidation component of degradation as temperature is ramped during analysis. On the other hand, if oxygen is consumed at a rate exceeding its replacement, then decreasing the air purge rate increases the thermal component of degradation, resulting in an increase in *OT* similar to the results noted above for analysis by TGA.

The decline in *OT* from corresponding analyses by DSC and P−DSC analyses of SME−1, shown graphically for individual scans in figure 1, suggests that the increasing pressure was more dominant than the decrease in air purge rate. Although not presented graphically in the present work, all mixtures of SME−1 with added antioxidants (loadings = 0 to 5000 ppm), demonstrated lower *OT* values measured from dynamic mode P−DSC heating scans than those from corresponding DSC scans. Thus, under the conditions of this study, increasing pressure accelerated the rate of oxidation reaction despite a decrease in purge gas flowrate from DSC to P−DSC analyses. This observation indicates that P−DSC is better suited than conventional DSC for analyzing oxidative degradation reactions by non−isothermal thermal analyses.

Oxidation reactions in the measurement cell generally take place at or near the air−oil interface. Hence, the rate of reaction also depends on the total interfacial area of contact between bulk air and oil phases. Since purge gas and flowrate affect the total mass of oxygen available in bulk air phase, these conditions also affect the migration rate of oxygen to the reaction zone. This allows a reinterpretation of *OT* results for methyl oleate and SME−1 summarized in tables 1 and 2. Neglecting variations in air flowrate, the following observations were made: (1) TGA heating scans yielded little conclusive evidence for oxidation reactions taking place during analysis; (2) DSC scans exhibited generally lower *OT* values than TGA scans; (3) dynamic mode P−DSC scans showed generally lower *OT* values than DSC scans; and (4) in order of increasing total mass of air to oil ratios, TGA was less than DSC owing mostly to a decrease in sample mass (from 15 to 2.1 mg), and DSC was less than P−DSC owing to the increase in pressure (ambient to 2000 kPa). These results show increasing air−oil mass ratio accelerates the oxidation component of thermal−oxidative reactions by increasing the concentration of oxygen in contact with oil at the interface.

In contrast, an earlier study (Knothe and Dunn, 2003) showed that increasing air−oil mass ratio increases *OSI* of methyl oleate, a conclusion that suggests increasing the quantity of air relative to total oil mass increases oxidative stability. However, those *OSI* data were measured isothermally at 90°C, a temperature that was relatively low in comparison with the *OT* data shown in table 2. This suggested the presence of significant oxidative degradation under conditions of the *OSI* analyses. In addition, decreasing total oil mass relative to air for analysis of *OSI* reduces both the molar quantity of double bonds available for reaction and the total residence time for air bubbles as they pass through the heated oil. Both of these conditions effectively decelerate the rate of reaction for oxygen in contact with heated oil.

Oxidation reactions carried out at or near the air−oil interface depend on concentration driving forces for moving un−reacted molecules in the bulk phases to the reaction zone. During the early stages of an *OSI* analysis, oxygen and un−reacted oil concentrations in corresponding bulk phases are nearly constant and the rate of oxidation near the interface is nearly constant and relatively independent of total oil mass. Thus, the only portion of the overall oxidation reaction occurring during *OSI* analysis that can be affected by a decrease in air−oil mass ratio relates to those effects noted above for the presence of air bubbles in the heated bulk oil phase. In contrast, the absence of air bubbles in DSC or

Table 2. Results from non−isothermal differential scanning calorimetry (DSC) and pressurized−differential scanning calorimetry (P−DSC) analyses of FAME.[a]

		Conventional DSC[b]		Dynamic Mode P−DSC[c]	
FAME	Antioxidant	*OT* (°C)	R_F	*OT* (°C)	R_F
Methyl oleate	None	168 ±3.9	1.0000	164 ±2.4	1.0000
Methyl linoleate	None	109 ±1.1	0.8662	82.4 ±0.26	0.8132
SME−1	None	136 ±2.0	0.9284	116 ±1.4	0.8939
SME−1	α−Tocopherol[d]	143 ±3.4	0.9431	128 ±1.6	0.9199
SME−1	TBHQ[d]	167 ±1.7	0.9983	137 ±1.0	0.9412
SME−2	None	143 ±6.3	0.9431	133 ±1.1	0.9282

[a] SME−1 = soybean oil FAME from Interchem, SME−2 = soybean oil FAME from Ag Environmental Products. *OT* = onset temperature, R_F = ratio of sample *OT* to methyl oleate *OT*, and TBHQ = *tert*−butyl hydroquinone.
[b] DSC: air flowrate = 75 mL/min; ramp rate = 5°C/min.
[c] P−DSC: air flowrate = 35 mL/min; pressure = 2000 kPa; ramp rate = 5°C/min.
[d] Loading = 2000 ppm.

Table 3. Results from non–isothermal P–DSC analysis of FAME in dynamic and static modes.[a]

FAME	Antioxidant	Dynamic Mode P–DSC[b]		Static Mode P–DSC[c]	
		OT (°C)	R_F	*OT* (°C)	R_F
Methyl oleate	None	164 ±2.4	1.0000	159.2 ±0.56	1.0000
Methyl linoleate	None	82.4 ±0.26	0.8132	128.2 ±0.47	0.9282
SME–1	None	116 ±1.4	0.8939	126 ±1.2	0.9224
SME–1	α–Tocopherol[d]	125.1 ±0.31	0.9137	134.2 ±0.74	0.9420
SME–1	TBHQ[d]	129 ±1.1	0.9233	139 ±1.2	0.9531
SME–1	BHA[d]	136.9 ±0.16	0.9408	146.3 ±0.63	0.9701
SME–1	BHT[d]	138.52 ±0.078	0.9446	141 ±1.7	0.9589
SME–1	Propyl gallate[d]	139.5 ±0.75	0.9469	142 ±2.2	0.9890
SME–2	None[d]	133 ±1.1	0.9282	148 ±1.3	0.9736

[a] BHA = *tert*–butyl–4–hydroxyanisole; BHT = 2,6–di–*tert*–butyl–4–methylphenol; propyl gallate = 3,4,5–trihydroxybenzoic acid propyl ester (see tables 1 and 2 for other abbreviations).
[b] Dynamic mode: air flowrate = 35 mL/min; pressure = 2000 kPa; ramp rate = 5°C/min.
[c] Static mode: closed system/no air flow; pressure = 2000 kPa; ramp rate = 5°C/min.
[d] Loading = 500 ppm.

P–DSC analysis means that the air–oil interface provides the only available location for reaction. If this is the case, then results from the current study show that decreasing the air–oil mass ratio decelerates the oxidative component of thermal–oxidative degradation during non–isothermal DSC and P–DSC heating scans.

Dynamic Mode P-DSC Versus Static Mode P-DSC

Results from dynamic and static mode P–DSC analyses of methyl oleate, methyl linoleate, SME–1, SME–2, and SME–1 treated with 500 ppm α–tocopherol, TBHQ, BHA, BHT, and propyl gallate are summarized in table 3. Corresponding R_F ratios defined by equation 1 are also listed. Analogous to the results listed in table 2, increasing the degree of unsaturation of FAME not treated with added antioxidant decreases *OT* from non–isothermal P–DSC scans in static mode. In addition, the observation that treating SME–1 with 500 ppm antioxidant generally increases *OT* supports the conclusion noted above that increasing oxidative stability coincides with an increasing *OT*. Results for SME–1 treated with α–tocopherol, TBHQ, BHA, BHT, and propyl gallate generally agreed with those reported in an earlier work (Dunn, 2005b).

Figure 3 is a graph of R_F corresponding to *OT* data from dynamic mode P–DSC heating scans versus R_F from static mode P–DSC scans. The $y = x$ line shows that nearly all FAME mixtures with or without antioxidants yielded dynamic mode results that were lower than static mode results. With the exception of methyl oleate, this effect is reflected for both *OT* and R_F data. Methyl oleate analyzed by dynamic mode P–DSC yielded *OT* values that were ~5°C higher than those analyzed by static mode P–DSC. Statistical comparison of mean *OT* values showed that nearly all FAME and SME–1 plus antioxidant mixtures deviated significantly ($P < 0.05$) between results for dynamic and static mode P–DSC. The only four exceptions were SME–1 plus 1000 ppm TBHQ, 5000 ppm BHA, 500 ppm propyl gallate, and 1000 ppm propyl gallate ($P = 0.15$ to 0.26).

The decrease in *OT* calculated from analysis of dynamic mode scans relative to those from static mode scans is illustrated graphically for individual P–DSC scans of untreated SME–1 in figure 1. As discussed above, the total mass of oxygen available for reaction influences oxidation during a heating scan. In general, the results listed in table 3 and figure 3 show that operating in dynamic mode with an air purge rate of 35 mL/min allows replacement of oxygen consumed by the reaction, accelerating oxidation during the scan and significantly reducing *OT* with respect to static mode P–DSC scans. Therefore, conducting heating scans in dynamic mode was more suitable than static mode with respect to analyzing oxidation of FAME by in non–isothermal P–DSC.

Least–squares linear regression of *OT* data corresponding to R_F data depicted in figure 3 yielded the following equation:

$$\begin{bmatrix} OT \text{ from} \\ \text{dynamic mode} \end{bmatrix} = 0.9 \begin{bmatrix} OT \text{ from} \\ \text{static mode} \end{bmatrix} - 2 \qquad (2)$$

The regression analysis yielded a relatively low coefficient of deviation ($R^2 = 0.77$) owing to significant scatter in the data. Although the slope of equation 2 was close to unity, paired two–sample Student's *t*–tests showed very little probability (<0.000001) for a direct correlation between mean *OT* values from dynamic and static mode P–DSC scans.

OSI Results

Results from oxidative stability instrument analysis of *OSI* isothermally at 60°C of methyl oleate, SME–1, SME–2,

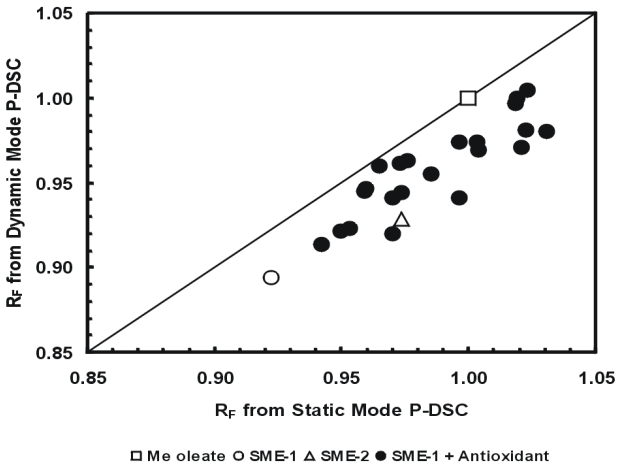

Figure 3. Response factor (R_F) results calculated from P–DSC analyses plotted as dynamic mode versus static mode (Me oleate = methyl oleate). Antioxidants were α–tocopherol, TBHQ (*tert*–butylhydroquinone), BHA (9% 2–*tert*–butyl–4–hydroxyanisole, 90% 3–*tert*–butyl–4–hydroxyanisole), BHT (99% 2,6–di–*tert*–butyl–4–methylphenol), and propyl gallate, each at loadings of 200 to 5000 ppm. See figures 1 and 2 for abbreviations.

and SME−1 treated with 200 and 500 ppm of α−tocopherol and TBHQ are summarized in table 4. Similar to presentation of results from conventional DSC and P−DSC scans, R_F ratios based on *OSI* data defined by the following equation are listed in table 4:

$$R_F = [OSI \text{ of sample}]/[OSI \text{ of methyl oleate}] \quad (3)$$

where *OSI* of sample and methyl oleate replicates were measured simultaneously in the oxidative stability instrument.

Consistent with results from non−isothermal DSC and P−DSC scans of FAME not treated by added antioxidants (see tables 2 and 3), the data in table 4 generally show that increasing the degree of unsaturation decreases oxidative stability, resulting in a decrease in *OSI*. In addition, increasing the oxidative stability of SME−1 by adding antioxidants increases *OSI*. Further, TBHQ was significantly more effective than α−tocopherol in increasing the oxidative stability of SME−1. These results are comparable to those for the *OT* data from DSC and P−DSC scans discussed above and agree with results reported in an earlier work (Dunn, 2005c). Finally, SME−2 without added antioxidant yielded an *OSI* that was significantly larger than that of SME−1 treated with α−tocopherol or 200 ppm TBHQ. As discussed above for the data from dynamic P−DSC scans, this result suggests that SME−1 was more harshly treated than SME−2 before its selection for the present study.

Correlation of OSI and Non−Isothermal P−DSC Results

Calculation of R_F ratios by equations 1 and 3 for corresponding samples allows direct comparison of results from isothermal *OSI* and non−isothermal conventional DSC and static and dynamic mode P−DSC analyses of oxidative stability. Based on the following seven data pairs, two−sample Student's *t*−tests were conducted: methyl oleate, SME−1, SME−1 plus α−tocopherol (two loadings), and SME−1 plus TBHQ (two loadings). Results from this comparison indicated that R_F from static and dynamic mode P−DSC have relatively high probabilities (0.75 and 0.79, respectively) favoring correlation to R_F from *OSI* results. On the other hand, R_F inferred from conventional DSC demonstrated no correlation ($P < 0.02$) to ratios from *OSI* results.

Polavka et al. (2005) and Šimon et al. (2000) studied dependence of oxidation induction period (*IP*) on temperature by correlating data from non−isothermal DSC and differential thermal analyses with results from isothermal oxidograph and Rancimat analyses. This correlation was expressed in the following Arrhenius−type equation:

Table 4. Results from oil stability index (*OSI*) analysis of FAME.[a]

FAME	Antioxidant	Loading (ppm)	*n*	*OSI*[b] (h)	R_F
Methyl oleate	None	0	2	140 ±3.5	1.0000
SME−1	None	0	3	7.2 ±0.30	0.0510
SME−1	α−Tocopherol	200	3	18.0 ±0.25	0.1285
SME−1	α−Tocopherol	500	3	30.7 ±0.44	0.2188
SME−1	TBHQ	200	3	33 ±1.1	0.2359
SME−1	TBHQ	500	3	146 ±1.7	1.0446
SME−2	None	0	2	53 ±1.3	0.3805

[a] R_F = ratio *OSI* of sample to *OSI* of methyl oleate, and *n* = number of replicate measurements (see table 2 for other abbreviations).

[b] *OSI* measured isothermally according to American Oil Chemists' Society test method Cd 12b−92 (see Dunn and Knothe, 2003); block temperature = 60°C.

$$IP = A \times \exp\{B/OT\} \quad (4)$$

where *A* and *B* are experimentally determined constants. If equation 4 is rewritten as follows:

$$\ln[OSI] = \log[A] + B/OT \quad (5)$$

where *OSI* = *IP*, then a plot of ln[*OSI*] versus OT^{-1} should yield a straight line if equation 5 is true.

Figure 4 is a plot of ln[*OSI*] versus OT^{-1} data for the seven data pairs statistically compared above where *OT* data were determined from dynamic mode P−DSC scans. Least−squares linear regression analysis of the data yields the following equation:

$$\ln[OSI] = 30 - 11{,}000/OT \quad (6)$$

which is represented by the solid line in figure 4. The degree of scatter in the data led to a relatively low coefficient of deviation ($R^2 = 0.45$) for equation 6. Omitting the data point for methyl oleate significantly improves the results by increasing R^2 to 0.83 and reducing standard error of the *y*−estimate (σ_y) from 0.97 to 0.58.

Similar regression with respect to *OT* data from static mode P−DSC scans yielded the following equation:

$$\ln[OSI] = 40 - 15{,}000/OT \quad (7)$$

where $R^2 = 0.38$ and $\sigma_y = 1.0$. Data pairs for SME−1 plus 500 and 1000 ppm TBHQ appeared as outliers for this analysis, and their omission increased R^2 to 0.89 and reduced σ_y to 0.35.

Overall, results from the present work do not exhibit a strong linear correlation based on equation 5 for *OT* data determined from non−isothermal static or dynamic P−DSC analyses. However, future research will be necessary to confirm this observation.

Conclusions

Results from non−isothermal TGA analyses of FAME under nitrogen and air purge gases were nearly indistinguish−

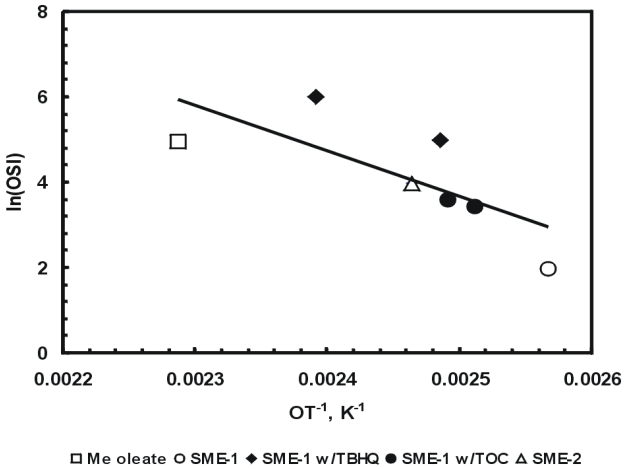

Figure 4. Correlation of oil stability index (*OSI*) measured at 60°C with *OT* data from dynamic mode P−DSC analyses plotted as ln(*OSI*) versus OT^{-1} (TOC = α−tocopherol). SME−1 treated with antioxidants TBHQ and TOC at loadings of 500 and 1000 ppm. Solid line corresponds to results from least−squares linear regression: slope = −11,000; intercept = 30; adjusted coefficient of deviation (R^2) = 0.45; and standard error of the *y*−estimate (σ_y) = 0.97. See figures 1, 2, and 3 for abbreviations.

able with respect to *OT* and other parameters. The total mass of oxygen present for 60 mL air/min at ambient pressure was not sufficient to cause measurable oxidation during non−isothermal heat scans.

Dynamic mode P−DSC heating scans yielded *OT* values that increased with relative oxidative stability, with the highest values being observed for methyl oleate.

Conventional DSC heating scans generally yielded *OT* values that were higher than those obtained from P−DSC scans. Conducting DSC scans at initially ambient air pressure meant that less oxygen was available for reaction, which resulted in a decreased oxygen component in the overall thermal−oxidative reaction.

Comparison of static and dynamic mode P−DSC heating scans showed that dynamic mode scans yielded lower *OT* values. This suggested that the oxidative component in the overall thermal−oxidative reaction was lower for static mode P−DSC. Overall, conducting scans in dynamic mode is more suitable than static mode for analyzing oxidation of FAME by in non−isothermal P−DSC.

Treating SME−1 with antioxidants increased oxidative stability, resulting in an increase in *OT* calculated from non−isothermal DSC and P−DSC heating scans.

Comparison of R_F data obtained from non−isothermal heating scans with those from isothermal *OSI* measurements demonstrated the highest degree of statistical correlation with respect to dynamic mode P−DSC.

In contrast to work reported by Polavka et al. (2005) and Šimon et al. (2000), results presented in the current work do not show a strong linear correlation with respect to ln[*OSI*] versus OT^{-1} with respect to results from either static or dynamic mode P−DSC scans.

ACKNOWLEDGEMENTS

Haifa Khoury, Brittney L. Mernick, and Kevin Steidley provided technical assistance for the experimental analyses conducted in this study. Paul Clayton helped guide modification of the TA model 2910 P−DSC for operation in dynamic mode.

REFERENCES

ASTM. 2003. D 6751: Standard specification for biodiesel fuel (B100) blend stock for distillate fuels. West Conshohocken, Pa.: American Society for Testing and Materials.

Bondioli, P., A. Gasparoli, A. Lanzani, E. Fedeli, S. Veronese, and M. Sala. 1995. Storage stability of biodiesel. *J. American Oil Chem. Soc.* 72(6): 669−702.

Bondioli, P., A. Gasparoli, L. D. Bella, and S. Tagliabue. 2002. Evaluation of biodiesel storage stability using reference methods. *European J. Lipid Sci. Tech.* 104(12): 777−784.

Canakci, M., A. Monyem, and J. H. Van Gerpen. 1999. Accelerated oxidation process in biodiesel. *Trans. ASAE* 42(6): 1565−1572.

Clothier, P. Q. E., B. D. Aguda, A. Moise, and H. Pritchard. 1993. How do diesel−fuel ignition improvers work? *Chem. Soc. Rev.* 22(2): 101−108.

Dunn, R. O. 2000. Analysis of oxidative stability of methyl soyate by pressurized−differential scanning calorimetry. *Trans. ASAE* 43(5): 1203−1208.

Dunn, R. O. 2002. Effect of oxidation under accelerated conditions on fuel properties of methyl soyate (biodiesel). *J. American Oil Chem. Soc.* 79(9): 915−920.

Dunn, R. O. 2005a. Chapter 6.2: Cold weather properties and performance of biodiesel. In *The Biodiesel Handbook*, 83−121. G. Knothe, J. Krahl, and J. Van Gerpen, eds. Champaign, Ill.: AOCS Press.

Dunn, R. O. 2005b. Effect of antioxidants on the oxidative stability of methyl soyate (biodiesel). *Fuel Processing Tech.* 86(10): 1071−1085.

Dunn, R. O. 2005c. Oxidative stability of soybean oil fatty acid methyl esters by oil stability index (OSI). *J. American Oil Chem. Soc.* 82(5): 381−387.

Dunn, R. O., and M. O. Bagby. 1995. Low−temperature properties of triglyceride−based diesel fuels: Transesterified methyl esters and petroleum middle distillate/ester blends. *J. American Oil Chem. Soc.* 72: 895−904.

Dunn, R. O., and G. Knothe. 2003. Oxidative stability of biodiesel in blends with jet fuel by analysis of oil stability index. *J. American Oil Chem. Soc.* 80(10): 1047−1048.

Du Plessis, L. M., J. B. M. de Villiers, and W. H. van der Walt. 1985. Stability studies on methyl and ethyl fatty acid esters of sunflowerseed oil. *J. American Oil Chem. Soc.* 62(4): 748−752.

Gamelin, C. D., N. K. Dutta, N. R. Choudhury, D. Kehoe, and J. Matisons. 2002. Evaluation of kinetic parameters of thermal and oxidative decomposition of base oils by conventional, isothermal and modulated TGA, and pressure DSC. *Thermochim. Acta* 392−393: 357−369.

Gan, L. H., K. S. Ooi, L. M. Gan, and S. H. Groh. 1995. Effects of epoxidation on the thermal oxidative stabilities of fatty acid esters derived from palm olein. *J. American Oil Chem. Soc.* 72(4): 439−442.

Giles, H. H. 2003. Methods for assessing stability and cleanliness of liquid fuels. In *Significance of Tests for Petroleum Products*, 108−117. 7th ed. S. J. Rand, ed. West Conshohocken, Pa.: American Society for Testing and Materials.

Graboski, M. S., and R. L. McCormick. 1998. Combustion of fat and vegetable oil derived fuels in diesel engines. *Prog. Energy Combust. Sci.* 24: 125−164.

Gunstone, F. D. 1967. Chemical properties of fatty acids and their esters. In *An Introduction to the Chemistry and Biochemistry of Fatty Acids and Their Glycerides*, 83−137. London, U.K.: Chapman and Hall.

Keller, M. A., and C. S. Saba. 1998. Behavior of high temperature lubricants in a pressure differential scanning calorimeter. *Tribol. Trans.* 41(4): 586−592.

Knothe, G., and R. O. Dunn. 2001. Chapter 5: Biofuels derived from vegetable oils and fats. In *Oleochemical Manufacture and Applications*, 106−163. F. D. Gunstone and R. J. Hamilton, eds. Sheffield, U.K.: Sheffield Academic.

Knothe, G., and R. O. Dunn. 2003. Dependence of oil stability index of fatty compounds on their structure and concentration and presence of metals. *J. American Oil Chem. Soc.* 80(10): 1021−1026.

Krahl, J., M. Bahadir, A. Münack, L. Schumacher, and N. Elser. 1996a. Survey about biodiesel exhaust emissions and their environmental benefits. In *Proc. 3rd Liquid Fuel Conference: Liquid Fuel and Industrial Products from Renewable Resources*, 136−148. S. Cundiff, E. E. Gavett, C. Hansen, C. Peterson, M. A. Sanderson, H. Shapouri, and D. L. Van Dyne, eds. St. Joseph, Mich.: ASAE.

Krahl, J., J. Bünger, H.−E. Jeberien, K. Prieger, C. Schütt, A. Münack, and M. Bahadir. 1996b. Analysis of biodiesel exhaust emissions and determination of environmental and health effects. In *Proc. 3rd Liquid Fuel Conference: Liquid Fuel and Industrial Products from Renewable Resources*, 149−165. J. S. Cundiff, E. E. Gavett, C. Hansen, C. Peterson, M. A. Sanderson, H. Shapouri, and D. L. Van Dyne, eds. St. Joseph, Mich.: ASAE.

Lacoste, F., and L. Lagardere. 2003. Quality parameters evolution during biodiesel oxidation using Rancimat test. *European J. Lipid Sci. Tech.* 105(3−4): 149−155.

Litwinienko, G., and T. Kasprzyska−Guttman. 2000. Study on autoxidation kinetics of fat components by differential scanning calorimetry: 2. Unsaturated fatty acids and their esters. *Ind. Eng. Chem. Res.* 39(1): 13−17.

Litwinienko, G., A. Daniluk, and T. Kasprzyska−Guttman. 1999. A differential scanning calorimetry study on the oxidation of C_{12}−C_{18} saturated fatty acids and their esters. *J. American Oil Chem. Soc.* 76(6): 655−657.

Litwinienko, G., A. Daniluk, and T. Kasprzyska−Guttman. 2000. Study on autoxidation kinetics of fats by differential scanning calorimetry: 1. Saturated C_{12}−C_{18} fatty acids and their esters. *Ind. Eng. Chem. Res.* 39(1): 7−12.

Mittelbach, M., and S. Schober. 2003. The influence of antioxidants on the oxidation stability of biodiesel. *J. American Oil Chem. Soc.* 80(8): 817−823.

Miyashita, K., and T. Takagi. 1988. Autoxidation rates of various esters of sunflower oil and linoleic acid. *J. American Oil Chem. Soc.* 65(7): 1156−1158.

Monyem, A., M. Canakci, and J. H. Van Gerpen. 2000. Investigation of biodiesel thermal stability under simulated in−use conditions. *Applied Eng. in Agric.* 16(4): 373−378.

Polavka, J., J. Paligová, J. Cvengroš, and P. Šimon. 2005. Oxidation stability of methyl esters studied by differential thermal analyses and Rancimat. *J. American Oil Chem. Soc.* 82(7): 519−524.

Prankl, H. 2002. High biodiesel quality required by European standards. *European J. Lipid Sci. Tech.* 104(6): 371−375.

Riga, A. T., R. Collins, and G. Mlachak. 1998. Oxidative behavior of polymers by thermogravimetric analysis, differential thermal analysis, and pressure differential scanning calorimetry. *Thermochim. Acta* 324: 135−149.

Sharma, B. K., and A. J. Stipanovic. 2003. Development of a new oxidation stability test method for lubricating oils using high−pressure differential scanning calorimetry. *Thermochim. Acta* 402: 1−18.

Sheehan, J., V. Camobreco, J. Duffield, M. Graboski, and H. Shapouri. 1998. Final report: Life cycle inventory of biodiesel and petroleum diesel for use in an urban bus. NREL−SR−580−24089. Golden, Colo.: National Renewable Energy Laboratory.

Šimon, P., L'. Kolman, I. Niklová, and Š. Schmidt. 2000. Analysis of the induction period of oxidation of edible oils by differential scanning calorimetry. *J. American Oil Chem. Soc.* 77(6): 639−642.

Stavinoha, L. L., and S. Howell. 1999. Paper No. 1999−01−3520: Potential analytical methods for stability testing of biodiesel and biodiesel blends. In *SAE Spec. Publ. SP−1482: Alternative Fuels 1999*, 79−83. Warrendale, Pa.: Society of Automotive Engineers.

Stavinoha, L. L., and K. S. Kline. 2001. Report: Oxidation stability of methyl soyates − Modified ASTM D 5304 and D 6186 for biodiesel B100. Washington, D.C.: U.S. Army, TACOM, TARDEC, National Automotive Center.

Thompson, J. C., C. L. Peterson, D. L. Reece, and S. M. Beck. 1998. Two−year study with methyl and ethyl esters of rapeseed. *Trans. ASAE* 41(4): 931−939.

U.S. EPA. 2002. *A Comprehensive Analysis of Biodiesel Impacts on Exhaust Emissions*. EPA420−P−02−001. Washington, D.C.: U.S. Environmental Protection Agency, Office of Transportation and Air Quality, Assessment and Standards Division.

Van Gerpen, J. H. 1996. Cetane number testing of biodiesel. In *Proc. 3rd Liquid Fuel Conference: Liquid Fuel and Industrial Products from Renewable Resources*, 197−206. J. S. Cundiff, E. E. Gavett, C. Hansen, C. Peterson, M. A. Sanderson, H. Shapouri, and D. L. Van Dyne, eds. St. Joseph, Mich.: ASAE.

Van Gerpen, J. H., S. Soylu, and M. E. Tat. 1996. Paper No. 996134: Evaluation of the lubricity of soybean oil−based additives in diesel fuel. In *Proc. Annual International Meeting of the ASAE*. St. Joseph, Mich.: ASAE.

Westbrook, S. R. 2003. Fuels for land use and marine diesel engines and for non−aviation gas turbines. In *Significance of Tests for Petroleum Products*, 63−81. 7th ed. S. J. Rand, ed. West Conshohocken, Pa.: American Society for Testing and Materials.

Yao, J. 1997. Evaluation of sodium acetylacetonate as a synergist for arylamine antioxidants in synthetic lubricants. *Tribol. Intl.* 30(11): 795−799.

Zeman, A., V. Becker, and K. Peper. 1993. Deposit formation in aero engines: Investigation by pressure differential scanning calorimetry (PDSC). *Thermochim. Acta* 219: 305−313.

Zeman, A., A. Sprengel, D. Niedermeier, and M. Späth. 1995. Biodegradable lubricants: Studies on thermo−oxidation of metal−working and hydraulic fluids by differential scanning calorimetry (DSC). *Thermochim. Acta* 268: 9−15.

NOMENCLATURE

BHA = *tert*−butyl−4−hydroxyanisole
BHT = 2,6−di−*tert*−butyl−4−methylphenol
DSC = differential scanning calorimetry (conventional mode)
FAME = fatty acid methyl esters
GC = gas chromatography
IP = induction period
OSI = oil stability index
OT = oxidation onset temperature, determined from non−isothermal TGA, DSC, or P−DSC heating scans
P−DSC = pressurized−differential scanning calorimetry (static or dynamic mode)
R^2 = coefficient of deviation, from regression analysis
R_F = response factor, ratio of *OSI* or *OT* of sample to corresponding data for methyl oleate (see eqs. 1 and 3)
SME = soybean oil FAME
σ_y = standard error of the *y*−estimate, from regression analysis
TBHQ = *tert*−butylhydroquinone
TGA = thermogravimetric analysis